Baku State University: Journal of Physics & Space Sciences, **2024**, v1 (3), p. 03-10

journal homepage: http://bsuj.bsu.edu.az/en

Laser ablation Undo thin films

Maarif A. Jafarov*, Huseyn M. Mamedov,
Vusal U. Mammadov, Elshan F. Nasirov

Baku State University, Baku, Azerbaijan

Received 18-Jul-2024; Accepted 30-Aug-2024
DOI: https://doi.org/10.30546/209501.2024.1.3.003

Abstract

Zinc cadmium oxide (ZnCdO) synthesis of zinc-oxide-based nanomaterials with specific properties is a great challenge due to its excellent industrial applications. We report the production of zinc cadmium oxide thin films as a first step for developing a n-ZnCdO/p-Si heterojunction.

Keywords: *thin films; zinc cadmium oxide; laser ablation; optical properties*
PACS: 71.55.Gs; 78.20.-e; 85.30.-z; 85.60.Dw

1. Introduction

Over the past decades, the advancement in the field of thin films technology paved the road for development of various semiconductor-based devices [1–3]. In this context, zinc oxide (ZnCdO) thin films and nanostructures attracted a great interest, owing to their unique properties such as large exciton binding energy (60 meV), direct wide-bang gap of about 3.37 eV at room temperature, high optical transparency in the visible region, low electrical resistivity, as well as high electrochemical stability, high electron mobility, nontoxicity, and abundance in nature, therefore being used in a wide range of application in the UV region of optoelectronic devices [4–6].

Moreover, ZnCdO-based nanomaterials can be considered as promising candidates for solar cells, gas sensors, laser diodes, and so on. ZnCdO films can be grown by several physical and chemical methods such as sputtering, chemical vapor deposition, sol-gel method, molecular beam epitaxy, and pulsed laser deposition on a

*e-mail: maarif.jafarov@mail.ru; ORCID ID: 000-0001-7483-4882.

wide range of substrates [7–9]. Taking into consideration all these approaches, in the present context of using green technologies, not all techniques are considered clean, especially wet-chemical methods for which the chemical residues involved proved to be harmful. Thus, new approaches should be considered and refined. Laser ablation has been a well-studied techniques since its early days and it has been showing the premises to be implemented to produce n-type ZnCdO thin films.

Pulsed laser deposition (PLD) has been studied and employed as a relatively simple and reliable technique for depositing a wide range of materials for novel applications [10–12]. Due to its versatility, flexibility, and process speed, the technique has emerged as a suitable production method for almost any material, ranging from simple materials (metals, oxides, semiconductors) to complex multilayer and multicomponent compounds and even biological materials with stoichiometric transfer of materials from the target [13]. Being a physical vapor deposition process that can be carried out in high vacuum, atmosphere, and even in liquids, the technique has attracted high interest in many fields. Among other advantages, the PLD technique offers the possibility of producing good quality transparent films [14].

It is well established that pure undoped ZnCdO films generally indicate *n*-type conduction. Silicon is a suitable material for integration in optoelectronic devices due to its low cost. Our final aim is to create a heterojunction of n-ZnCdO/p-Si that has the potential of being integrated in a wide range of applications such as gas sensors, solar cells, photodiodes, and many others [15]. As an initial step towards our goal, in this study we focus on the preparation of highly oriented ZnCdO thin films by pulsed laser deposition at relatively low substrate temperatures. We take advantage of the PLD technique, namely, by the possibility of controlling the elemental composition of the deposited thin films much better than using other methods. The structure, morphology, composition, and optical properties of the obtained films are characterized by means of X-ray diffraction (XRD), scanning electron microscopy (SEM), and energy-dispersive X-ray spectroscopy (EDS) UV-VIS measurements.

2. Materials and Methods

The ZnCdO thin films were deposited on commercially available silicon wafers (cut 5 5 mm) using an ArF laser with a wavelength of 193 nm (Coherent COMPex Pro 205F) by ablating a sintered Zn,Cd target in high purity NaOH solution. The laser repetition rate can be varied from 1 to 50 Hz, and the energy per pulse can be set in the range of 10 to 400 mJ. For this study, the laser was operated at a frequency of 10 Hz with a constant power of 300 mJ.

The surface of the target is repolished after each deposition to keep it flat. In all cases, the distance between target and substrate was kept constant at 5 cm. The schematic diagram of the experimental setup is depicted in Figure 1.

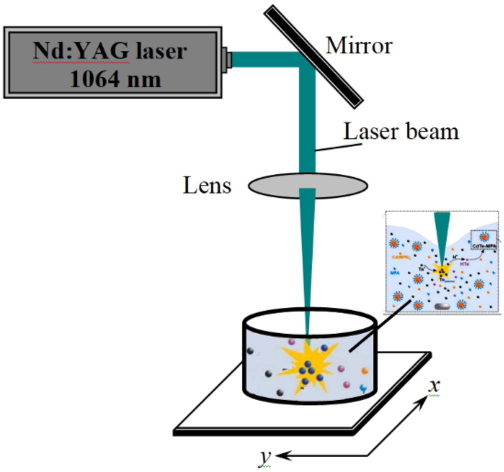

Fig. 1. Schematic representation of the automated pulsed laser deposition system.

The crystallographic structure of the deposited thin films was characterized by X-ray diffraction (XRD) using a Shimadzu LabX XRD 6000 Diffractometer system with a CuK_α (λ = 1.5406 Å) source. The surface morphology was investigated using scanning electron microscopy (SEM) (Quanta 450, FEI,). The samples were analyzed as they were, the system being able to image conductive and non-conductive samples as well without any prior preparation. The elemental composition analysis was performed with an energy dispersive X-ray spectrometry (EDS) module coupled with an SEM machine (EDAX,). Absorbance measurements were obtained with a UV-VIS spectrophotometer (Thermo Scientific Evolution 300,). Each of the above-mentioned measurements were performed on at least three of the samples for each experiment.

3. Results and Discussions

The crystalline phase and orientation of the ZnCdO thin films was determined by XRD measurements using Scherrer's formula [28] to calculate the crystalline size:

$$D = \frac{k\lambda}{\beta cos\theta},$$

where the constant $k = 0.94$ is the shape factor, λ is the wavelength of X-rays 1.5406 Å for Cu K_α, ϑ is the Bragg's angle, and β is the full width at half maximum. From the diffraction patterns, a good crystalline behavior is revealed with a preferential growth of the thin films on the (002) plane, suggesting that there are no secondary phases, as seen from Figure 2. The inset of the figure depicts the crystalline phase and orientation of the Si substrate as measured by XRD. The position of the

(002) is consistent with the values from literature: PDF card no 00-005-0664.

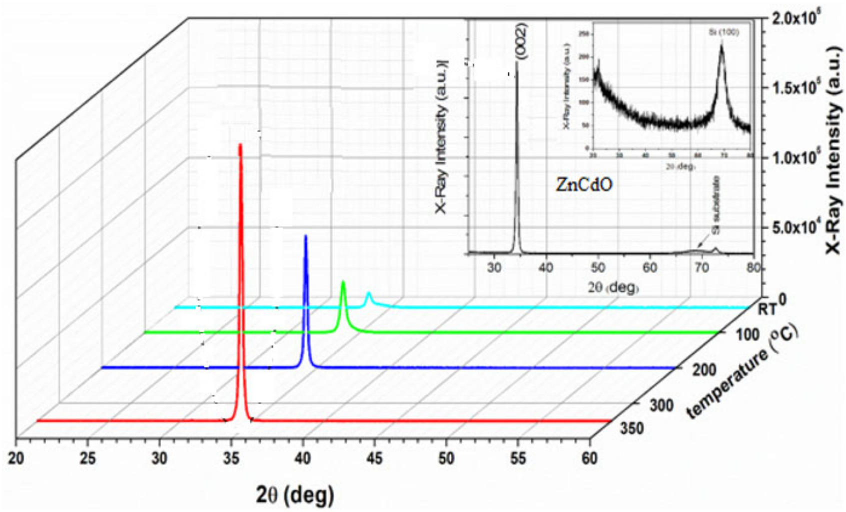

Fig. 2. XRD pattern for ZnCdO thin films and Si substrate (inset).

Knowing the structure of the (002) diffraction peaks, the crystalline plane distance d, the lattice constant c, and the strain ε of the ZnCdO thin films are calculated. The crystalline distance d for the index (002) is given by the Bragg formula:

$$d = \frac{\lambda}{2sin\theta} \quad (1)$$

and the lattice constant c is equal to 2 d. The strain ε in the films along the c-axis is calculated by the formula:

$$\varepsilon = \frac{c - c_0}{c_0}, \quad (2)$$

where c_0 is the unstrained lattice constant and has a value of 0.5205 nm for bulk ZnCdO. The positive value for the strain ε depicts a very low tensile strain of ZnCdO thin films approaching an almost stress-free ZnCdO. The intensity of the (002) diffraction peak increases as a function of substrate temperature and is revealing an improvement of the film's crystallinity. The film deposited at room temperature exhibits a lower crystallinity compared with those deposited at about 350°C. The annealing of different layers induced changes in the crystalline lattice constant of ZnCdO, which changed the tensile stress in the ZnCdO thin films. A shift toward a high angle of the XRD peak is observed due to the narrowing of the distance d between the lattice planes. As a result, preferentially c-plane-oriented, highly crystalline ZnCdO thin films are produced.

Figure 3 shows the surface of the thin films obtained for different substrate temperatures. It is clearly seen that this is a crucial factor that dictates the morphology, as found for other deposition methods as well such as sputtering—the ratio between the temperature of the substrate and the melting temperature of the deposited material influences the porosity of the deposited films [16].

EDS spectra of the ZnCdO thin films are presented in Figure 4. For each of the samples, Zn and O are the main constituents, with no trace of impurities (within the detection limit of EDS) with respect to substrate temperature used during PLD deposition. For the samples deposited at 350°C, the EDS spectrum also shows an increase in the Si signal related with the substrate. In this case, as seen from the SEM micrographs of the deposited material, the substrate detection indicates an increase in the porosity, thus, the electron beam not only reaches the film but also the substrate through the formed pores. In the studied conditions, all the films have approximately the same thickness, the deposition rate being similar. From the spectra presented in Figure 4, a quantification of the elements or oxide ratios can be performed automatically by the software (TEAMS ver. 4.1, EDAX). For the studied conditions, the average relative elemental concentrations estimated from the spectra are also shown in Figure 4.

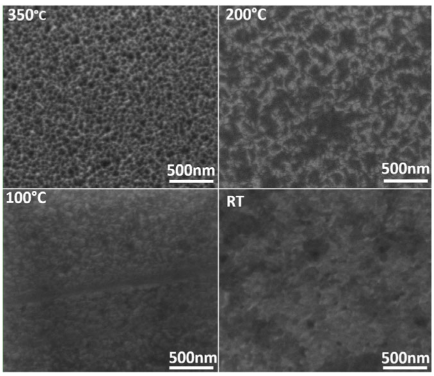

Fig. 3. SEM images of ZnCdO thin films for different deposition temperatures.

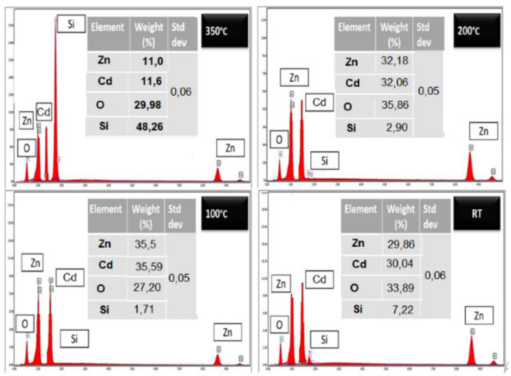

Fig. 4. EDS spectra of deposited ZnCdO thin films with corresponding relative elemental composition estimated from the spectra.

The optical absorption of the ZnCdO thin films was measured at room temperature using a UV-visible spectrophotometer within the range of 300 to 1100 nm. In Figure 5, the absorption spectra for ZnCdO thin films deposited at substrate temperatures of 350°C, 200°C, 100°C, and room temperature are presented. All the films exhibited a sharp absorption edge in the UV region at about 390 nm. Using the absorbance data, the direct transition band gap energies (E_g) were calculated based on Tauc's equation.

By plotting $(\alpha h\nu)^2$ versus the incident photon energy, the Tauc's plots are obtained, all the data being presented in Figure 5. By regressing to zero the linear portion of the $(\alpha h\nu)^2$ from Tauc plot, the energy band gap of the thin films is found.

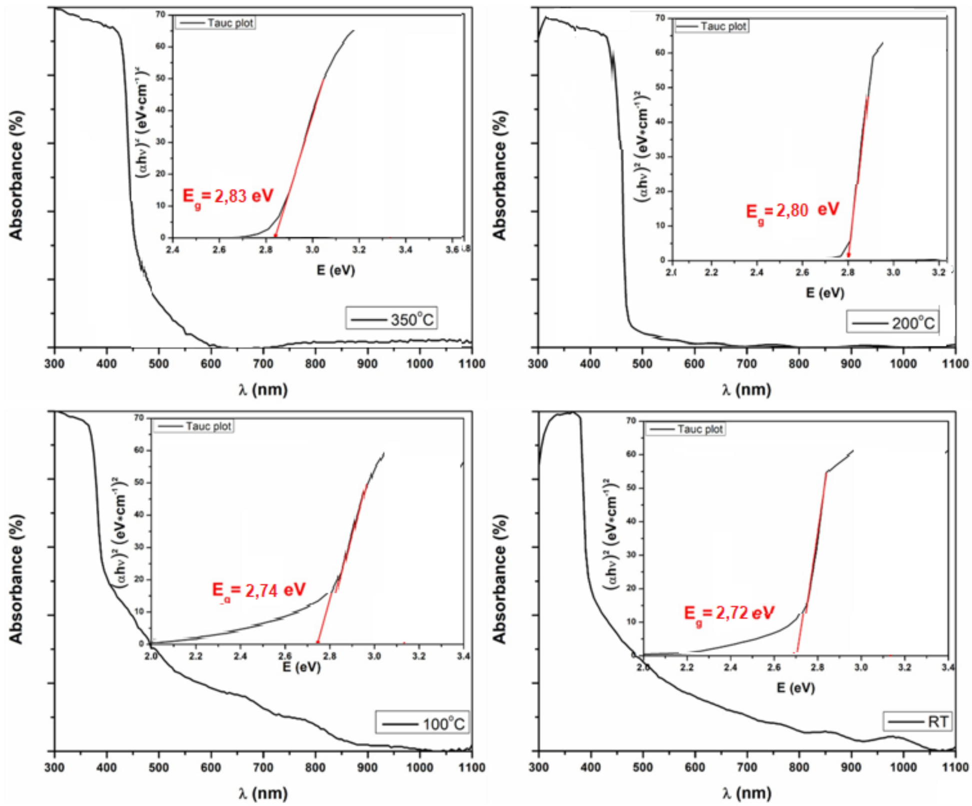

Fig. 5. Absorbance spectra of the zinc oxide thin films. Insets show Tauc plots employed for evaluating optical band gap energies of the thin films.

The values obtained were as follows: 3.32 eV, 3.25 eV, 3.13 eV, and 3.12 eV for the films deposited at 350°C, 200°C, 100°C, and room temperature, respectively. Compared to the value of 3.37 eV for bulk ZnCdO, the obtained values of the energy gap are slightly smaller for the films deposited at temperatures lower than 300°C as a consequence of various defects and zinc and/or oxygen vacancies present in the lattice of ZnCdO. As for the higher deposition temperature, it is clearly seen that the energy band gap is approaching the ideal value for bulk ZnCdO (~3.7 eV) [18]. This conclusion supports the improvement of the crystallinity of the thin films as seen from the XRD measurements earlier discussed.

4. Conclusions

Preferentially c-plane-oriented, highly crystalline ZnCdO thin films were obtained using pulsed laser deposition of a ZnCdO target in oxygen atmosphere as a first step in the development of an n-ZnCdO/p-Si heterojunction for applications. The dependence of the thin films structure and properties was observed as a function of the substrate temperature. The crystallinity increased for the thin films with the increasing temperature from room temperature to 350°C. The same behavior was observed for the band gap that changed from 3.12 eV at room temperature, close to the ideal value for the highest substrate temperature studied, with a value of 3.32 eV.

References

[1] Di Mauro, A.; Fragala, M.E.; Privitera, V.; Impellizzeri, G. ZnCdO for application in photocatalysis: From thin films to nanostructures. *Mat. Sci. Semicond. Process.* **2017**, *69*, 44–51.

[2] Laurenti, M.; Cauda, V. Porous Zinc Oxide Thin Films: Synthesis Approaches and Applications. *Coatings* **2018**, *8*, 67.

[3] Moezzi, A.; McDonagh, A.M.; Cortie, M.B. Zinc oxide particles: Synthesis, properties and applications. *Chem. Eng. J.* **2012**, *185–186*, 1–22.

[4] Jiang, Z.; Soltanian, S.; Gholamkhass, B.; Aljaafari, A.; Servati, P. Light-soaking free organic photovoltaic devices with sol–gel deposited ZnCdO and AZO electron transport layers. *RSC Adv.* **2018**, *8*, 36542–36548.

[5] Winantyo, R.; Murakami, K. ZnCdO Nanorods Formation for Dye-Sensitized Solar Cells Applications. *Int. J. Technol.* **2017**, *8*, 1462–1469.

[6] Morales, C.; Leinen, D.; del Campo, A.; Ares, J.R.; Sanchez, C.; Flege, J.I.; Gutierrez, A.; Preito, P.; Soriano, L. Growth and characterization of ZnCdO thin films at low temperatures: From room temperature to 120 °C. *J. Alloys Compd.* **2021**, *884*, 161056.

[7] Habibi, A.; Vatandoust, L.; Aref, S.M.; Naghshara, H. Formation of high performance nanostructured ZnCdO thin films as a function of annealing temperature: Structural and optical properties. *Surf. Interfaces* **2020**, *21*, 100723.

[8] Ogugua, S.N.; Ntwaeaborwa, O.M.; Swart, H.C. Latest development on pulsed laser deposited thin films for advanced luminescence applications. *Coatings* **2020**, *10*, 1078.

[9] Simdar, M.; Mousavi, S.S.; Sajad, B.; Hassani, F. Distinctive ZnCdO film's structures and morphologies for different modes of heating substrate. *Mater. Lett.* **2021**, *297*, 129914.

[10] Das, D.; Karmakar, L. Optimization of Si doping in ZnCdO thin films and fabrication of n-ZnCdO:Si/p-Si heterojunction solar cells. *J. Alloys Compd.* **2020**, *824*, 153902.

[11] Nguyen, V.H.; Resende, J.; Jimenez, C.; Deschanvres, J.L.; Carroy, P.; Munoz, D.; Bellet, D.; Munoz-Rojas, D. Deposition of ZnCdO based thin films by atmospheric pressure spatial atomic layer deposition for application in solar cells. *J. Renew. Sustain. Energy*

2017, *9*, 021203.

[12] Rasool, A.; Santhosh Kumar, M.C.; Mamat, M.H.; Gopalakrishnan, C.; Amiruddin, R. Analysis on different detection mechanisms involved in ZnCdO-based phtotodetector and photodiodes. *J. Mater. Sci. Mater. Electron.* **2020**, *31*, 7100–7113.

[13] Wen-Cheun Au, B.; Chan, K.-Y.; Sin, Y.-K.; Ng, Z.-N. Hot-point probe measurements of N-type and P-type ZnCdO films. *Microelectron. Int.* **2017**, *34*, 30–34.

[14] Ali, G.M. Performance analysis of planar Schottky photodiode based on nanostructured ZnCdO thin film grown by three different techniques. *J. Alloys Compd.* **2020**, *831*, 154859.

[15] Ortiz, T.; Conde, C.; Khan, T.M.; Hussain, B. Thickness uniformity and optical/structural evaluation of RF sputtered ZnCdO thin films for solar cell and other device applications. *Appl. Phys. A* **2017**, *123*, 280.

[16] Laurenti, M.; Canavese, G.; Sacco, A.; Fontana, M.; Bejtka, K.; Castellino, M.; Pirri, C.F.; Cauda, V. Nanobranched ZnCdO structure: P-type doping induces piezoelectric voltage generation and ferroelectric-photovoltaic effect. *Adv. Mater.* **2015**, *27*, 4218–4223.

[17] Lackner, J.M.; Waldhauser, W.; Alamanou, A.; Teichert, C.; Schmied, F.; Major, L.; Major, B. Mechanisms of self-assembling topography formation in low-temperature vacuum deposition of inorganic coatings on polymer surfaces. *Bull. Pol. Acad. Sci. Tech. Sci.* **2010**, *58*, 281–294.

[18] Zhao, Y.; Jiang, Y.; Fang, Y. The influence of substrate temperature on ZnCdO thin films prepared by PLD technique. *J. Cryst. Growth* **2007**, *307*, 278–282.